LION Navigator for Transfer to GEO Using Electric Propulsion

Mark Hartrampf, Hannes Filippi, Peter A. Krauss – *Airbus DS GmbH, Germany*
mark.hartrampf@airbus.com, hannes.filippi@airbus.com, peter.a.krauss@airbus.com
Oliver Montenbruck – *DLR-GSOC, Germany*, oliver.montenbruck@dlr.de
Eveline Gottzein – *University Stuttgart, Germany*, eveline.gottzein@airbus.com

BIOGRAPHY

Mark Hartrampf is a Systems Engineer at Airbus Defence and Space in Ottobrunn, Germany. After graduating in aerospace engineering at Stuttgart University in 2000, he joined Daimler aerospace (now part of Airbus). Following several years in AOCS development, he became project manager for space borne electronics products before joining the development of the next generation LION Navigator GNSS receiver as Systems Engineer.

Hannes Filippi works in spacecraft navigation using GNSS at Airbus Defence and Space in Ottobrunn, Germany. He studied Applied Physics at the University of Innsbruck, Austria, has a M.Sc. in Technology from Helsinki University of Technology, Finland, and a M.Sc. in Space Technology from Luleå Tekniska Universitet, Sweden.

Peter A. Krauss received his doctoral degree in engineering from the Technical University of Munich (Germany) in 1995. As a systems engineer at Airbus Defence and Space he is developing mainly new electronic products for satellites, like on board computers, GNSS receivers, and timing subsystems.

Oliver Montenbruck is head of the GNSS Technology and Navigation Group at DLR's German Space Operations Center. His research activities comprise spaceborne GNSS, formation flying, and precise orbit determination as well as new GNSS signals and constellations. Oliver Montenbruck chairs the Multi-GNSS Working Group of the International GPS Service and is a lecturer at Technische Universität München.

Eveline Gottzein studied Electrical and Control Engineering and Mathematics and Physics at Technical Universities in Dresden and Darmstadt, received her doctoral degree from Technical University, Munich. Since 1993, she is scientific consultant to Airbus Defence and Space for spacecraft navigation based on GNSS and optical sensors. Professor at University Stuttgart, E. Gottzein is also an AIAA and IFAC Fellow.

ABSTRACT

GNSS space receivers are widely used for onboard autonomous navigation of spacecraft platforms in low Earth orbit. Navigation by GNSS up to geosynchronous altitude was made possible through the introduction of a Space Service Volume which defines signal strength up to geosynchronous altitude. For Galileo, similar definitions are under consideration. On this basis onboard autonomous navigation for commercial communication satellites became a realistic possibility, too. Transfer to geostationary orbit is still fully depending on classical RF tracking by ground station for orbit determination. With electrical propulsion, the transfer duration extends to several months. As a consequence onboard autonomous navigation by satellite navigation has become of commercial interest.

A GNSS navigation receiver on a spacecraft on transfer orbit has to cope with extreme signal conditions from very low (at perigee) to very high (at super-synchronous apogee) altitude, which is far above the constellation satellites. At this altitude only very rare and weak signals that spill over the limb of the earth can be used. An additional difficulty is the varying spacecraft orientation which is not nadir pointing, as is commonly assumed, but is varying according to the demands of optimal attitude guidance laws and power requirements. By using both GPS and Galileo together the availability of navigation signals is increased.

The paper describes the design process to determine basic parameters e.g. number and orientation of receive antennas, receiver parameters like C/N_0 thresholds, and navigation procedures.

Detailed simulations are presented for selected parts of the transfer arc using verified models of the navigation receiver.

Finally the geostationary transfer capabilities of the space-borne LION Navigator GNSS receiver are demonstrated in a closed-loop real time test environment under RF stimulation.

INTRODUCTION

With the rapidly increasing number of geosynchronous communications satellites, onboard autonomous navigation by GNSS for satellites on geosynchronous station

became an interesting goal of receiver development. This was supported by the introduction of the Space Service Volume (SSV) starting with GPS III.

With the advance of electrical propulsion replacing chemical propulsion in the final stage, the transfer time to reach geosynchronous altitude after launch is extended from a few days to several months. This development stimulated interest in onboard autonomous navigation in the transfer phase with the goal to simplify procedures and finally to replace the classical RF tracking by ground station.

The paper describes the main features of the Airbus Defence and Space LION Navigator GNSS receiver and gives performance predictions based on integrated system tests for Low Earth Orbit (LEO), Geosynchronous Orbit (GEO), and Geosynchronous Transfer Orbit (GTO) using electrical propulsion.

SPECIFIC CHALLENGES OF GTO AND ELECTRICAL PROPULSION

Background

GPS was originally designed for terrestrial users and is used successfully on many satellites in LEO, where visibility conditions and signal strength are similar. Satellites in LEO typically have an upward, to the zenith looking, receive (Rx) antenna.

With an increasing demand on worldwide communications the number of satellites in GEO increases too. Onboard autonomous navigation by GPS for GEO satellites thus becomes a key goal of space-borne GNSS receiver development. Figure 1 shows the geometric relationship between a geosynchronous user spacecraft (S/C) and the Space Vehicles (SVs) in the GPS constellation.

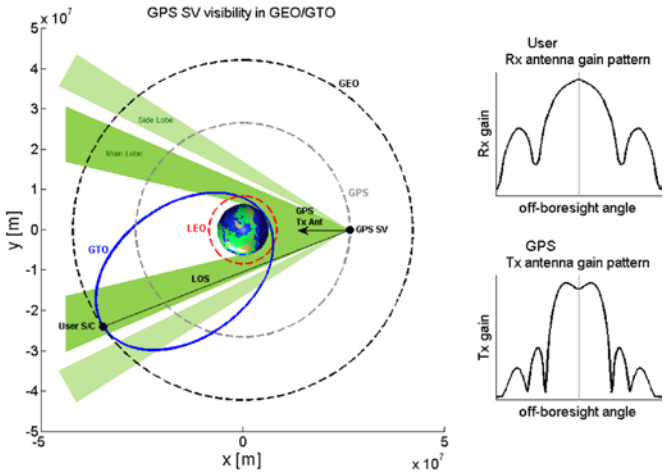

Figure 1: GPS SV visibility in GEO/GTO.

Satellites on geosynchronous altitude are flying above the GPS constellation. To receive signals that spill around the rim of the earth, the Rx antenna of a user satellite in GEO must point downwards to the earth (Nadir direction). To receive this main beam spill-over requires a high gain Rx antenna on the user to compensate the increased path loss [12]. The path length from a GPS SV to a user satellite in GEO is approx. 67 488 km (13,9°off bore sight). This corresponds to a path loss of -167,57 dB. In comparison, the path length to a GPS SV from a user in a 500 km earth orbit is approx. 19 689 km (0° off bore sight), resulting in a path loss of-156,88 dB, which is 10,7 dB more received power . Satellites in GEO orbit require a high gain receive antenna to compensate for the extra loss [01][05].

Satellites in transfer orbits transverse both the Terrestrial Service Volume (TSV) and the Space Service Volume SSV) [01], and, in case of Super Synchronous Transfer (SST), reach altitudes even beyond GEO. For launch by Falcon 9 (Space X) the apogee altitude of ~72000 km is used for fuel optimal inclination correction [04].

The electrical signal environment, which is unexplored so far and the use of GNSS in a way they were not designed for, present new challenges on receiver hardware and software design.
Here, only the most challenging ones, which require new procedures and developments, are listed:

- Sparse visibility, few satellites are visible only in the small field of view of the main beam spill-over,
- Weak signals due to the long distance between user and constellation satellites, e.g. 68000 km for satellites in GEO,
- Interruption by frequent gaps, where no GNSS signals are received,
- Interference from in-band RF disturbances from Earth, and onboard sources,
- Acquisition and tracking of false signals caused by the existence of numerous signals over greatly varying strength,
- “Near/Far effects” that could lead to saturation of the GNSS receiver by excessive C/N_0.

Airbus Defence and Space’s LION Navigator – taking into account those challenges and making use of modern GNSS signals – provides a solution for all satellite missions ranging from high performance LEO applications with a position accuracy of better than 1 m Root Mean Square (RMS) to geosynchronous satellites with a position accuracy of better than 20 m (RMS). More detail on LEO and GEO performances is provided in the following chapters.

Figure 1 also shows that side lobes are present but have much lower signal strength. Even worse, the signal quality is badly characterized so far and probably varies from GPS/Galileo generation to generation. Effects like code group delay, polarization mismatch, etc., prohibit the use of side lobes for performance prediction and specification until these properties are sufficiently well determined, [08], [09], [10], and [11].

As described by the Space Service Volume, the GPS III ICD IS-GPS-200H [17] guarantees Signal-in-Space (SIS) performance up to geosynchronous altitude for all modern GPS signals for the main lobe only. The current constellation with 28 active satellites is assumed in the present simulations (31 minus 3 GPS block II-A) For Galileo the constellation data are based on Galileo OS SIS ICD Issue 1, Revision 1, September 2010 [18].

Transfer Orbits to GEO

Characteristic transfer orbits to GEO are shown in Figure 2, c.f. [06] and [07].

The transfer orbit to GEO depends on the type of launch vehicle and launch location. The transfer is up to now conventionally performed by chemical thrusters, e.g. in case of Ariane 5 using an apogee motor of 400 N thrust. It takes only a few orbits and 3 to 4 thrust maneuvers to reach the desired orbital position in a sequence of Hohmann transfers. Typical for the transfer are long free-flying arcs, which require that the vehicle is inertially pointed to expose the solar generators, which are fixed to the S/C body, towards the Sun. An important alternative is the Super Synchronous Transfer Orbit SSTO (Falcon 9 by Space X), where the high apogee altitude is used for efficient inclination correction.

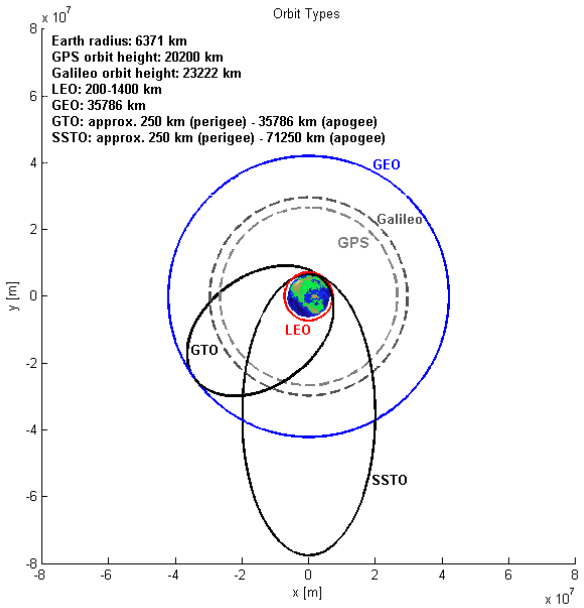

Figure 2: Orbit types: Low Earth Orbit (LEO), Geostationary Orbit (GEO), Geostationary Transfer Orbit (GTO), Super-Synchronous Transfer Orbit (SSTO).

The situation changes drastically with the use of electrical propulsion for orbit injection and on- orbit station keeping. Electrical propulsion is an interesting alternative to chemical propulsion because of the much higher specific impulse (vacuum Isp ~1680s) which results in considerable savings of launch mass. The price for this is the much lower thrust (~ 2 thrusters of 0.29 N each) of the electrical thrusters and consequently much longer transfer duration.

For an Ariane V GTO launch, Erb et. al. in [06] calculate the transfer duration to 90 days (124 to 126 revolutions), and Feuerborn et. al. in [07] calculate even up to some hundred days. Under this condition, it takes several hundred orbits for the user S/C to reach its final geosynchronous position.

The low thrust requires, that the thrusters are nearly continuously operated and that the vehicle is guided through a difficult environment, shared with many other spacecraft. Particularly challenging are low altitudes (< 900 km) and the altitude of GEO belt crossing, which is populated with many highly valuable operational communications satellites. To avoid interference with active telecom S/C in their GEO slots the GEO belt with an extension of +/- 75 km in north/south direction and +/- 35 km in radial direction is declared a protected region, only to be entered for insertion into the assigned box.

Other constraints come from the consideration of eclipses, requirements on Sun aspects angles, and constraints from attitude control system like blinding of sensors and limitations on attitude rates.

Under all these constraints the optimum thrust direction has to be translated into attitude guidance commands. The orientation is commonly described by quaternions in an Earth Centered Inertial (ECI) reference frame. The Rx antennas are fixed to the vehicle. Antenna orientation is described in body fixed coordinate system. From a GNSS navigation perspective, the navigation system has to be prepared to cope with greatly varying visibility conditions. This concerns geometrical distribution as well as signal strength. Varying vehicle attitude along the trajectory to align the thrust vector in the optimal direction is an additional challenge in case of electrical propulsion (EP).

A Generic Approach to Navigation System Design

Understanding the environment is key to designing a good navigation system for the sparse measurement environment up to GEO altitude and beyond [10]. This is the first time, that an onboard autonomous navigation system has to be designed for vehicles that operate below and above GNSS constellation altitudes

The following key parameters are selected to describe judge the navigation environment on transfer trajectories:

- Signal geometrical visibility: Geometrical visibility sets the limit to what is possible theoretically,
- Carrier to noise density ratio C/N_0: Signal power indicates how many of the geometrically visible satellites could actually be tracked under the limitations of the receiver. This “electrical visibility” sets the performance limits for a well-designed navigation filter.
- Signal outages: Gaps, where less than two GNSS satellites are visible by the receiver antenna. These gaps are caused by the unfavorable distribution of SVs in the constellations and have to

be bridged by propagation of highly accurate orbit models in the navigation part of the receiver.

Fortunately, the physical environment for satellites in Earth orbit is very well known [16], and can nowadays be modelled onboard with great accuracy thanks to powerful onboard processors. This knowledge is essential for navigation in the difficult environment of orbits beyond the constellations altitudes.

A sequential estimator or Kalman filter is implemented for onboard autonomous position and velocity determination, based on an orbit model and highly accurate force models of geopotential, gravitational attraction of moon and Sun, solar wind, and air drag. The Kalman filter is updated every time when two or more GPS or Galileo satellites are visible providing quasi-instantaneous update of state information with each measurement. Pseudo-range differences are used to eliminate common errors like receiver clock biases and make the Kalman filter robust.

Modelling errors are expected for air drag from residual atmosphere, and solar radiation pressure. A considerable source of error is the uncertainty in modeling thrust vector magnitude and direction. In the future, the Kalman filter will be extended to better deal with these perturbations.

Knee and intersection altitudes, and antenna orientation

So far, antennas pointing to the zenith, i.e. away from the Earth, are used for satellites in earth low orbit and nadir pointing antennas, i.e. to the center of the Earth, for satellites in GEO orbits. Stanton et al. in [02] investigated geometrical visibility as a function of orbit altitude for satellites with nadir and zenith Rx antennas for different apertures (half beam width) of transmit (Tx) antennas. Figure 3 shows the average number of GPS SVs in view for nadir and zenith Rx antennas of 90° aperture and a Tx antenna half beam width of 23.5°. Both curves intersect at about 2100 km. Stanton et al. show in [02] that the intersection point is independent from the Tx antenna aperture (for realistic half beam width). At intersection the average number of SVs in view by each Rx antenna is about 8.5°.

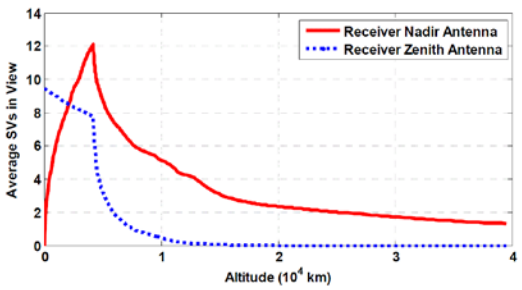

Figure 3: Average GPS space vehicles (SVs) in view (Replica from [02]).

More important are the distinct knees at about 4100 km, which move to higher altitudes when the Tx antenna aperture is increased. At knee altitude, the maximum average number of 12 SVs is visible by a nadir antenna for the half beam width of 23.5°.
For the GPS L5 signal with 26° half beam width the visibility increases to 13 and remains higher than for 23.5° with increasing altitude, improving visibility in the region above 4100 km in general.

Knee altitudes for GPS and Galileo signals and Rx nadir/zenith antennas' aperture of 85° and 90°are summarized in Table 1. For the more realistic 85° aperture angle, the knee altitudes are about 40 to 50 km higher [13].

Table 1: Knee altitude for Rx antenna aperture of 85° and 90°, c.f. [02] and [13].

	L1	E1	L5	E5
Half Beam Width, Tx antenna	23°	22°	26°	26°
Rx antenna 90°	4007 km	4710 km	5273 km	6598 km
Rx antenna 85°	4047 km	4753 km	5318 km	6647 km

Surprisingly, visibility by a nadir antenna starts at very low altitude, e.g. below perigee altitudes of some transfer orbits. Four or more SVs are visible in average by nadir antenna between 500 and about 13000 km, two or more between roughly 300 and about 25000 km.

As described earlier, navigation is performed based on sequential estimation by a Kalman filter. Updates are performed based on pseudo range differences requiring only a minimum of two visible SVs. This suggests that the only gain of having a zenith antenna in addition to a nadir antenna is in the visibility around perigee under ideal circumstances. But in the unrealistic case of a vehicle flying exactly in Local Vertical Local Horizontal (LVLH) reference frame, one nadir antenna may be sufficient for on board autonomous navigation.

In reality, number and orientation of antennas has to be selected considering varying attitude guidance requirements in particular during electrical transfer. But also during chemical transfer long free flying orbital arcs occur in between Hohmann maneuvers, where the vehicle is kept Sun oriented for power generation and temperature management.

A Global Approach to Visibility and C/N_0 Requirements

Navigation accuracy depends on the geometrical and electrical visibility which is expressed over the transfer orbit by

- Percentage of time when two (four) or more SVs are visible [03],
- Number of outages,
- Outage duration,
- C/N_0 acquisition/ tracking limits.

The investigation is performed using signals in the L1 band. GPS L1 and Galileo E1 are evaluated for two transfer trajectories to GEO.

GNSS Navigation in GTO

As reference, a typical Ariane 5 GTO is considered having a perigee at 234 km, an apogee at 35988.90 km, and an inclination of 5.97°. The geosynchronous target orbit has to be reached permitting a tolerance of up to 0.1° in inclination and +/- 36 km in radial direction, which gives some indication for the required measurement accuracy (at least one order of magnitude better.

The visibility analysis is performed assuming main lobes only for one Rx antenna pointing in nadir direction. For calculating average visibility 6 different start times, equally spaced are considered, [13], [17], [18]

Sample results showing GNSS satellite visibility over one orbit for GPS L1 and Galileo E1 and a specific start time are given in Figure 4, Figure 5, and Figure 6.

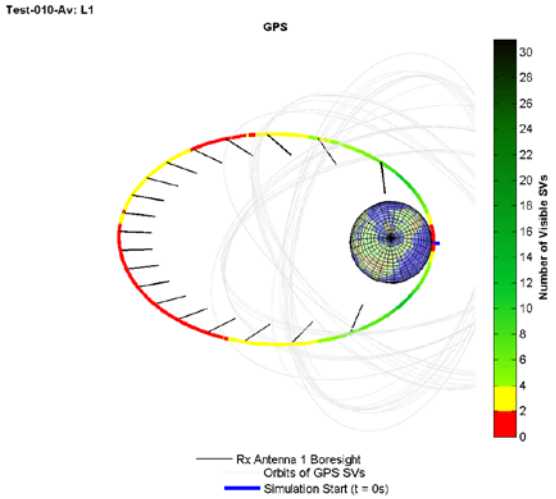

Figure 4: GPS SV visibility for L1, on a typical Ariane 5 GTO with nadir-pointing Rx antenna [13].

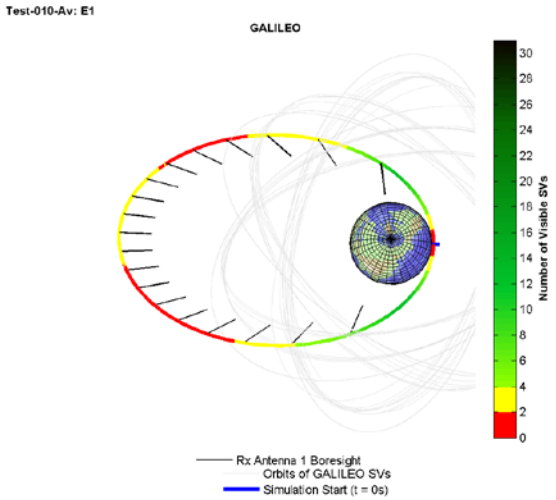

Figure 5: Galileo SV visibility for E1, on a typical Ariane 5 GTO with nadir-pointing Rx antenna [13].

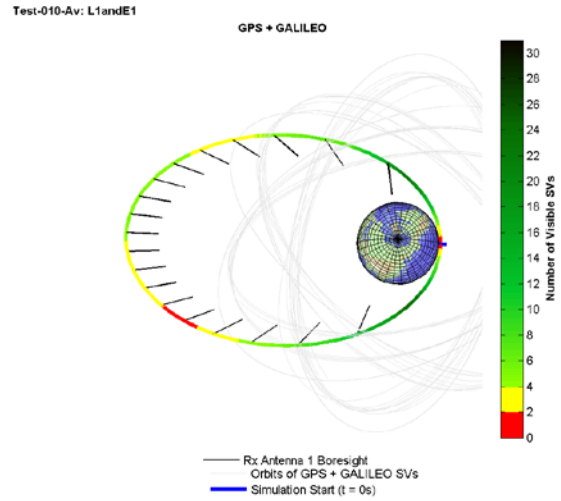

Figure 6: GPS + Galileo SV visibility for L1 + E1, on a typical Ariane 5 GTO with nadir-pointing Rx antenna [13].

The evaluation of average visibility over altitude in Figure 7 and Figure 8 confirm the knee from Figure 3.

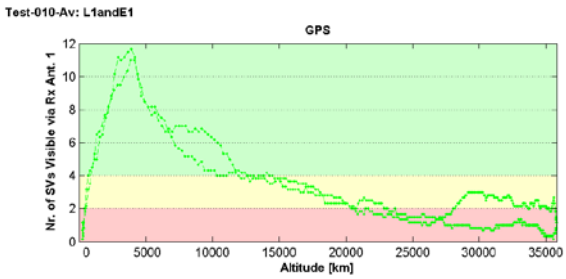

Figure 7: GPS SV visibility over user S/C altitude for a typical Ariane 5 GTO with nadir-pointing Rx antenna [13].

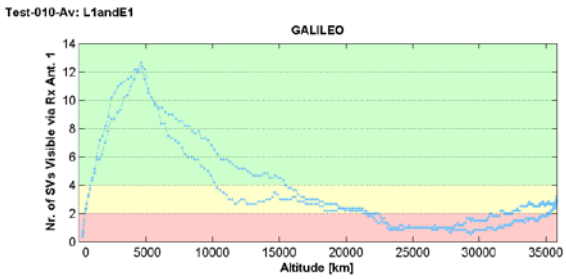

Figure 8: Galileo SV visibility over user S/C altitude for a typical Ariane 5 GTO with nadir-pointing Rx antenna [13].

Figure 9 for L1 and Figure 10 for E1 show how the geometrical visibility is influenced by the acquisition and tracking limits of the receiver. Despite the C/N_0 limit of 22 dB-Hz, the number of visible SVs stays the same most of the time. Galileo is affected more than GPS. Around the perigee, visibility is poor for both constellations and even drops below two as to be expected. But this lack of visibility is overcome by the increase of perigee altitude to > 300 km in the first few revolutions.

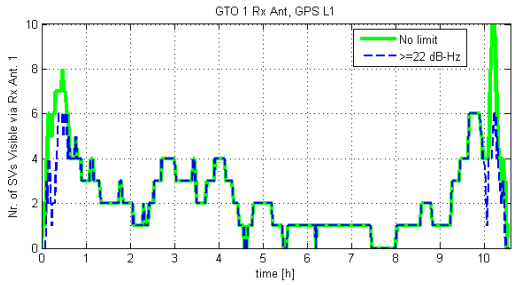

Figure 9: GPS SV visibility vs acquisition/tracking limit (22 dB-Hz), for a typical Ariane 5 GTO with nadir-pointing Rx antenna [13].

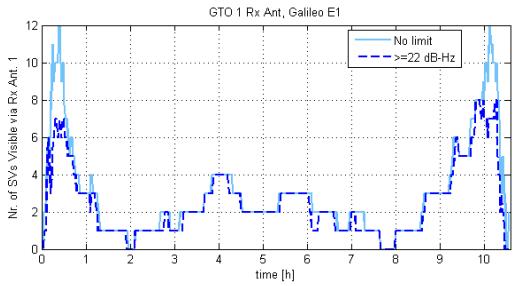

Figure 10: Galileo SV visibility vs acquisition/tracking limit (22 dB-Hz), for a typical Ariane 5 GTO with nadir-pointing Rx antenna [13].

Figure 11 and Figure 12 show histograms of received C/N_0 values. The main part of signals is distributed between 20 and 48 dB-Hz. The averaged mean C/N_0 values are nearly the same for GPS L1 (33.75 dB-Hz) and Galileo E1 (34.70 dB-Hz). For GPS L1, 22 dB-Hz are an adequate acquisition and tracking limit, while visibility of Galileo E1 would benefit from a somewhat lower limit.

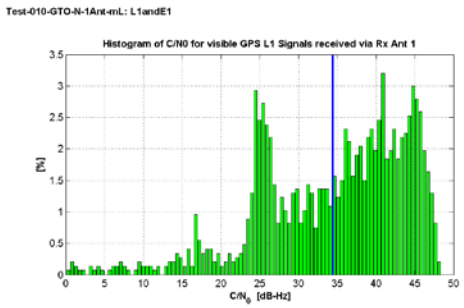

Figure 11: Histogram of C/N_0 values for visible GPS SVs (L1), for a typical Ariane 5 GTO with nadir-pointing Rx antenna [13].

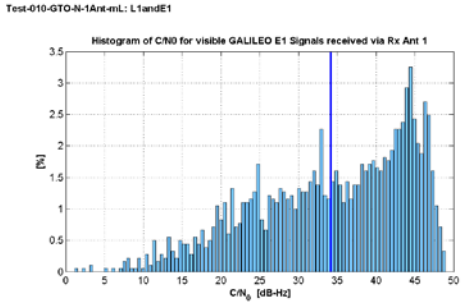

Figure 12: Histogram of C/N_0 values for visible Galileo SVs (E1), for a typical Ariane 5 GTO with nadir-pointing Rx antenna [13].

Signal Outages and SV Visibility

The LION Navigator uses an extended Kalman filter, based on pseudo-range differences. A Kalman filter update occurs when at least two SVs of the same constellation are received. Any epoch with less than two SVs of the same constellation is counted as outage. Table 2 show signal outages at GTO (orbit period approx. 10.5 h) for GPS L1, Galileo E1 and the combination for one nadir pointing Rx antenna.

Table 2: Signal outages over GTO for L1, E1, and L1+E1 (GTO with nadir Rx antenna) [13].

	GPS L1	Galileo E1	L1+E1
Number outages	5.33	7.17	5.33
duration min [min.]	2.50	1.33	1.33
duration mean [min.]	49.13	30.66	10.05
duration max [min.]	160.67	89.50	30.33

According to Table 2, for GPS L1 the number of outages during one GTO is around two smaller than for Galileo. However, the mean outage duration of E1 is 30.66 min only and much shorter than the mean of 49.13 min of GPS L1. The minimum and maximum outage duration is much shorter for Galileo E1 too. The navigation solution of the LION Navigator relies on a highly accurate orbit propagator to predict position, velocity, and time during outages. Initial errors at the beginning of the outage phase will be propagated and grow into higher deviations from the actual state. The conclusion is that having more outages with shorter outage duration gives better results than having only a few very long outages. When GPS L1 and Galileo E1 are used the number of outages remains as low as for L1 only. The mean duration is very much reduced to only 10.05 min per orbit.

Table 3 summarizes visibility for at least two and at least four SVs. When GPS L1 and Galileo E1 are used simultaneously, the percentage of time with at least two SVs visible increases to 90.97%. This means that 90.97% of the time an update of the Kalman filter solution is possible.

Table 3: Two/four or more visible signals over GTO for L1, E1, and L1+E1 (GTO with nadir Rx antenna) [13].

SV Visibility	GPS L1	Galileo E1	L1+E1
≥ 2 SVs visible [% of time]	60.66 ±8.95	66.56±6.88	90.97±4.63
≥ 4 SVs visible [% of time]	25.54±9.64	25.04±4.65	57.56±8.91

Visibility by Zenith Antenna

Figure 13 and Figure 14 (above) demonstrate for GPS L1 and Galileo E1, respectively, that a zenith antenna improves visibility close to perigee only. The rapid drop of visible satellites is expected from Figure 13 and Figure 14 (below), which show the distinct knee in the number of visible satellites over orbit altitude. There are distinct knees for both signals (GPS L1 at about 3900 km, Galileo E1 at about 4700 km). Beyond 5000 km user altitude, the zenith antenna does not contribute to visibility anymore. The additional Rx antenna in zenith direction improves

the SV visibility by only 1-2 %. The gap around perigee depends on the perigee altitude and disappears at a perigee altitude of about 300 km. For the GTO under investigation (perigee 234 km), the outage at perigee amounts to 6-12 min.

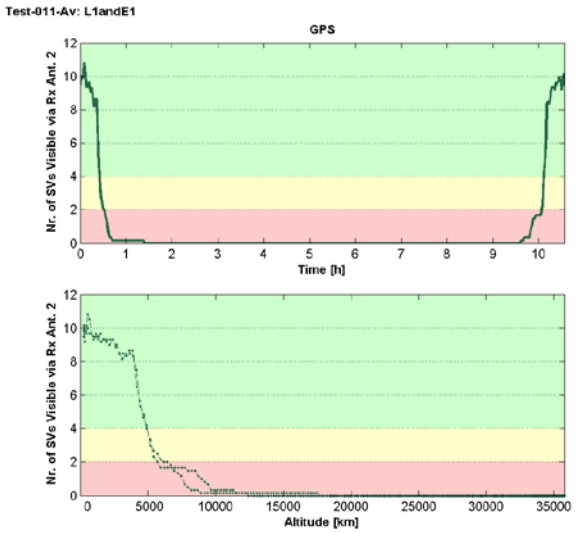

Figure 13: GPS SV visibility for zenith pointing Rx antenna on a typical Ariane 5 GTO, w.r.t. time (above), w.r.t. user S/C altitude (below) [13].

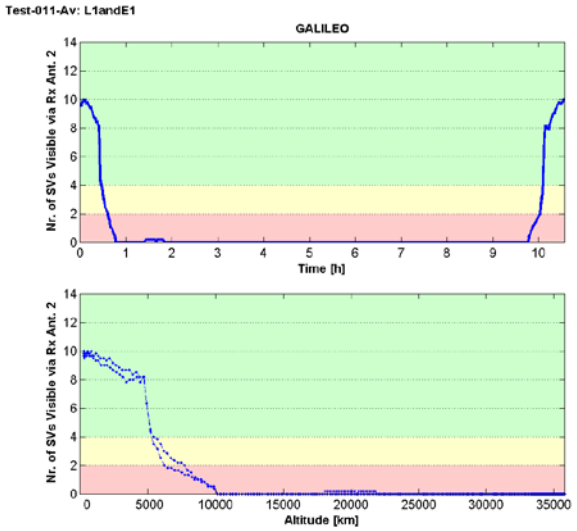

Figure 14: Galileo SV visibility for zenith pointing Rx antenna on a typical Ariane 5 GTO, w.r.t. time (above), w.r.t. user S/C altitude (below) [13].

Using GPS L5 and Galileo E5a in GTO

Similar to the GEO orbit [15], the signals in the L5/E5 frequency band also give better results for GTO. Table 4 shows that an improvement for all key figures is obtained by the use of L5/E5. The improvement is the results of wider half beam angles (26°) and higher transmit power (GPS L5 minimum received power -157.9 dB W). Almost complete coverage of the orbit with at least two visible SVs is possible using solely Galileo E5a (95% coverage) or GPS L5 (74% coverage).

Table 4: GTO visibility using frequency band L5/E5 [19].

Visibility	**GPS L5**	**Galileo E5**
≥ 2 visible [% of time]	75.41	96.90
Number outages	4.83	3.50
Outage duration min [min.]	3.83	1.33
Outage duration mean [min.]	33.47	5.79
Outage duration max [min.]	88.83	11.83

Other useful features of signals L5/E5a are:

- Higher code chipping rates (10.23 MHz), therefore higher processing gain,
- Data-less (Pilot) components, allow tracking in lower signal C/N_0 conditions by PLL,
- Secondary codes, reduce cross correlation between signals (side lobes!) and impact of narrowband interference.

An important advantage in case of a nadir antenna at perigee is expected from the increased robustness against narrow band interference.

Navigation on transfer orbit using electrical propulsion

As already mentioned, results for electrical transfer vary not only depending on the target orbit and the launch vehicle but also for different parts of the launch trajectory. The main reason for deviation, e.g. for an Ariane chemical GTO from the corresponding electrical GTO is to be explained by the attitude guidance program, resulting from the optimal transfer trajectory, which was selected in the special case. Results presented are from an early part of a realistic transfer orbit, which is close to GTO with an apogee of 35595 km and a perigee of 185 km. Orbit and realistic attitude maneuvers used in the simulation were provided by the Astos Solutions GmbH, Germany [13]. EP transfer orbit and orientation of Rx antennas are shown in Figure 15 and Figure 16. Baseline for the tests are two antennas either in orthogonal [+y, +x] or anti-parallel [+y,-y] mounting w.r.t. S/C body frame [13]17. The bore sight in y-direction constantly points in the orbit plane but not necessarily in the nadir direction.

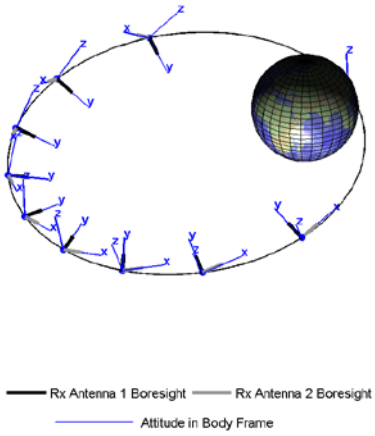

Figure 15: Realistic EP transfer orbit with user S/C orientation using two orthogonal Rx antennas (S/C

body frame +x and +y axis). Scenario provided by Astos Solutions GmbH, Germany [13].

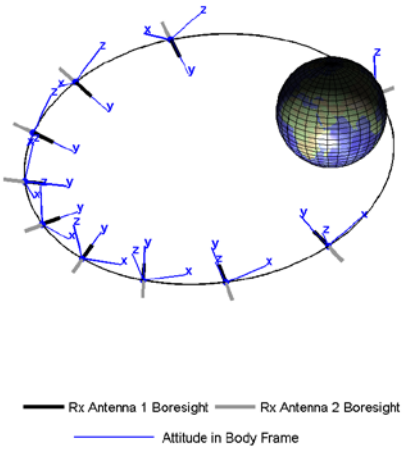

Figure 16: Realistic EP transfer orbit with user S/C orientation using two anti-parallel Rx antennas (S/C body frame +y and -y axis). Scenario provided by Astos Solutions GmbH, Germany [13].

Figure 17 and Figure 18 show the visibility of L1 and E1 signals for both antenna mountings (anti-parallel and orthogonal, one set of start conditions only). Figure 17 and Figure 18 show that the distribution of outages is similar for both antenna arrangements.

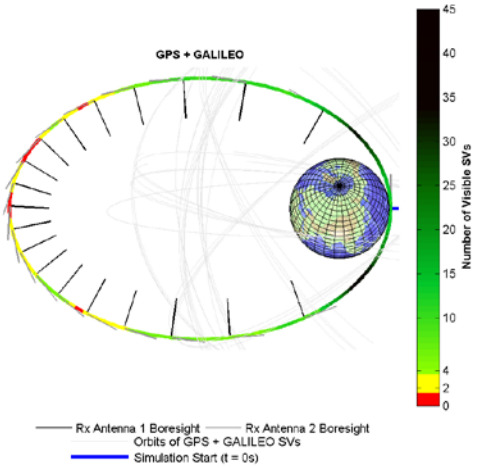

Figure 17: GPS and Galileo SV visibility for L1 + E1 on a realistic EP transfer orbit with user S/C orientation using two orthogonal Rx antennas [13].

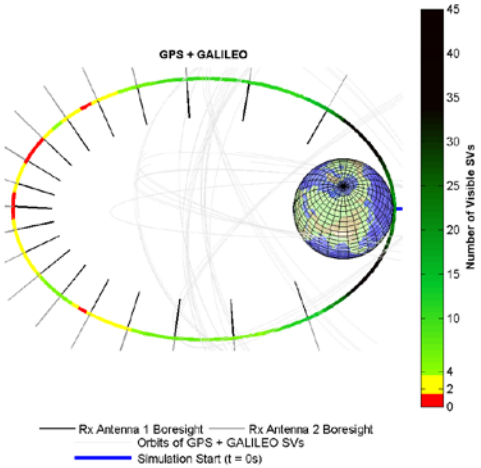

Figure 18: GPS and Galileo SV visibility for L1 + E1 on a realistic EP transfer orbit with user S/C orientation using two anti-parallel Rx antennas [13].

The observation is supported by results in Table 5. The values are displayed for GPS only, Galileo only, and GPS and Galileo together and show a remarkable result. Although, outages are differently distributed, the overall percentage of outage time and visibility is equal for the two antenna arrangements. This leads to the conclusion, that visibility is mainly determined by the antenna in the plus y direction and the second antenna doesn't improve the visibility. This supports the earlier finding, that a zenith antenna improves visibility only around perigee.

Table 5: Visibility for characteristic transfer trajectory for electrical propulsion using 2 Rx antennas [13].

Visibility	**Rx antennas' mounting**	**GPS L1**	**Galileo E1**	**L1+E1**
[%] of time with >2 SVs visible	Orthogonal	55.52	55.52	86.23
	Anti-parallel	55.52	55.52	86.23

Although the orbit chosen for the electrical transfer is similar to GTO, the comparison of Table 3 and Table 5 reveals that visibility is reduced in the case of electrical transfer. Here the Rx antenna is not strictly nadir pointing because the vehicle attitude has to follow the direction commanded by the optimal attitude guidance law.
Results in this section were obtained for geometrical visibility. Histograms in Figure 19 and Figure 20 permit the assumption, that visibility assuming a C/N_0 limit of 22 dB-Hz is comparable.

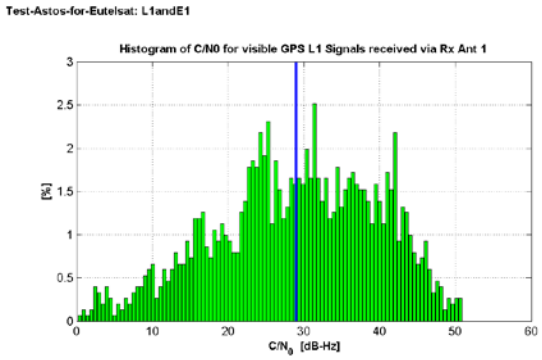

Figure 19: Histogram of GPS SV visibility for L1 for Rx antenna 1 [13].

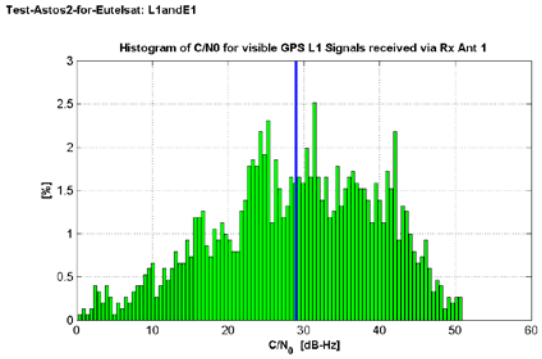

Figure 20: Histogram of Galileo SV visibility for E1 for Rx antenna 1 [13].

LION NAVIGATOR GNSS RECEIVER

LION Navigator Basics

The different challenges and restrictions of LEO and GEO orbit often lead to specific versions of space-borne receivers for these different types of orbits (e.g. the GEO specific variant of Airbus Defence and Space's MosaicGNSS receiver [21]). As described above, the geostationary transfer orbit incorporates both orbit types with additional challenges specific to the transfer orbit.

The goal of Airbus Defence and Space was to develop a space borne GNSS receiver product for Galileo and modernized GPS that can be used in any satellite orbit from LEO to GEO - including the challenging transfer to GEO – with the same hardware and software for all missions.

This development led to the current, fully space-qualified, LION Navigator (see [14], [15]), which is based on both, a next generation GNSS core supporting GPS and Galileo, and a powerful LEON-2 processor architecture. These two elements are combined in a single ASIC, the AGGA-4. The design goal was to provide 36 single frequency channels, which can be used for multi-frequency purposes. In addition, the LION Navigator hardware and software design is strictly modular in order to facilitate reuse, upgrading, and re-configuration [20].
The LION Navigator is designed to make at least use of the GPS signals L1, L2C, and L5 and of the Galileo signals E1, and E5a. As long as enough channels are available, all GPS and Galileo satellites in view will be tracked.

The LION Navigator demodulates the navigation data messages of the GPS and Galileo navigation signals and uses this information for determination of position, velocity, and time (PVT) through instant point-solution as well as through a dynamic Kalman filter solution. The goal was to reach in low Earth orbits sub-meter absolute position accuracy and a "Pulse-Per-Second (PPS)" timing accuracy of less than 30 ns (1-sigma).
The redundant flight model unit and the digital board are shown in the photos of Figure 21.

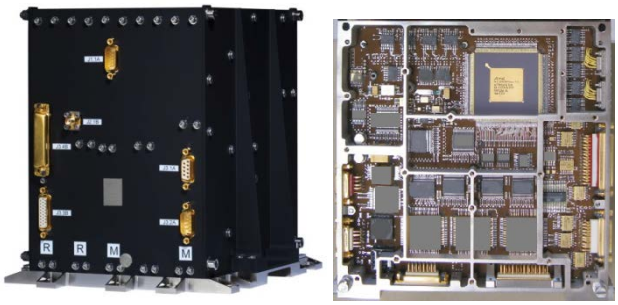

Figure 21: LION Navigator Flight Model and Digital Board

Hardware Overview

Figure 22 shows the hardware block diagram of LION Navigator, divided into an RF frame containing the RF front-ends and clock generation, the digital board for the base-band processing, and a separated power converter.
Centerpiece on the digital board is the AGGA-4, described in [26]. In the RF frame, the selection of the frequency band is done through a small number of external passive components inside the RF front-ends. Before entering the respective RF front-ends, a flexible RF distribution allows various configurations of feeding antenna RF signals to the RF front-ends.

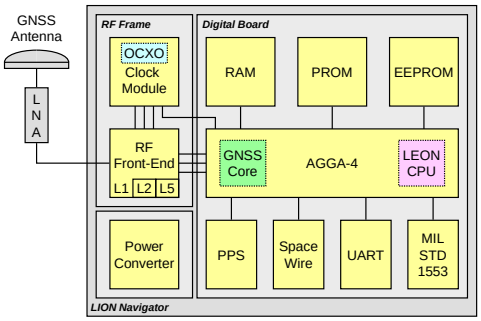

Figure 22: LION Navigator hardware modules.

Software Overview

The GNSS application of LION Navigator is subdivided into the application core and the application framework.
The application core comprises:

- the sensor module
- the navigation solution module
- the navigation planning module

The data flow within the application core is given in Figure 23 and further described below within the respective software modules.

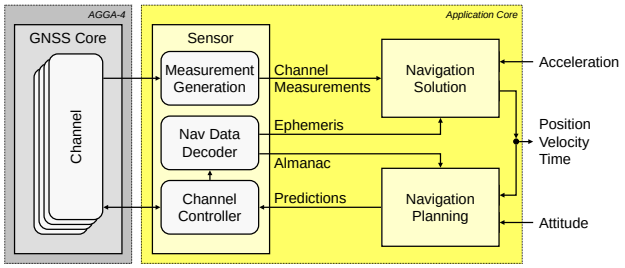

Figure 23: Data flow inside application core.

Sensor Module

The sensor module contains all functions needed to process the GNSS signals and to decode the included GNSS navigation messages. The sensor module is operating the GNSS core of the AGGA-4 [26].

Based on the predictions from the navigation planning module the sensor module applies different integration times for the signals in order to allow for tracking of signals with very large difference in signal-to-noise ratio at the same time as is often the case during the GTO.

Navigation Solution

The navigation solution module calculates the navigation solution on the data from the sensor module, considering also ionospheric and clock information. The result of the navigation solution consists of the position, velocity and time information of the user.

As shown in Figure 23, the navigation solution module may be informed about accelerations from thruster activities to improve the response of the Kalman filter. This is essential for the compensation of the continuous thrust of the electrical propulsion system in the electrical orbit raising case.

Navigation Planning

The navigation planning module performs the allocation of GNSS satellites to the sensor module. It uses information from the GNSS almanac data, the PVT from the navigation solution module, and information about the user satellite like antenna bore sight and attitude.

As shown in Figure 23 the navigation planning module should be informed about spacecraft attitude changes to improve the visibility prediction.

The LION Navigator uses RTEMS as the operating system. RTEMS is generally described in [27].

Real-Time Test Environment

For the test results presented below, the test environment shown in Figure 24 is used. This test environment is a result of many years of experience in closed loop real-time testing of GNSS receivers for space applications.

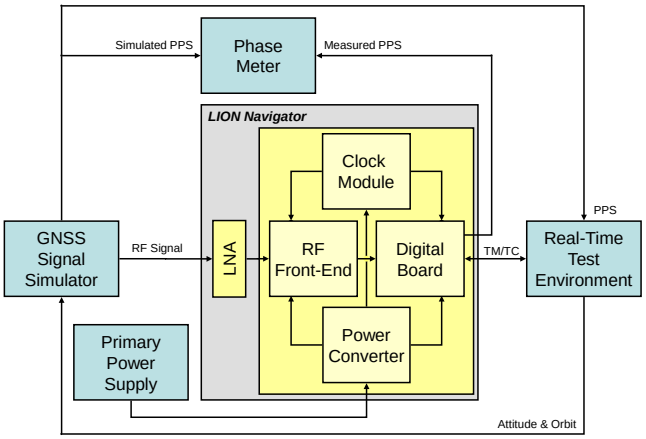

Figure 24: Test setup for integrated system tests.

A pre-computed reference scenario, known as "motion file", runs on the Spirent GNSS simulator. In parallel, the attitude & orbit maneuvers are commanded by TC messages to the GNSS receiver as they occur. The RF signal output from the Spirent simulator is fed directly into the LNA of the LION Navigator.

Afterwards, the generated and the calculated data received from the GNSS receiver can be compared, visualized and stored for further processing. The key features of the test environment are the following:

- Spirent GSS8000 Simulator with 3 x 12 channels for GPS, simulating L1, L2, and L5 and with 3 x 12 channels for Galileo, simulating E1, E5a, and E5b (E5b is not used be LION Navigator).
- Spacecraft simulation for user orbit and attitude, producing the motion file and the TC message list, considering the following external forces:
  - *Earth Gravitation:*
    The model used for the Earth gravitation is a JGM3 (Joint Gravity Model) of 70^{th} degree
  - *Sun and Moon Gravitation:*
    The Sun and Moon are considered as point masses and the Earth is not at rest.
  - *Atmospheric Drag and Solar Pressure:*
    In low orbits the atmospheric force (air drag) represents the largest non-gravitational perturbations. For the modelling of the atmospheric density a Harris-Priester density model is used. The acceleration of the satellite due to solar pressure is also considered for full illumination.
- Generation of automatic test sequences and automatic data analysis scripts.

Ionospheric and tropospheric errors as environmental effects are considered. The delay of the GNSS pseudo-ranges due to effects of the ionosphere is modelled in the Spirent Simulator. A constant vertical total electron content (VTEC) of $2 \cdot 10^{17}$ electrons/m^2 (= 20 TECU) has been selected for the used scenarios. As the troposphere is the lower atmosphere from the Earth surface to approximately 50 km, and only signals passing this small part of the atmosphere would be affected, the tropospheric effects are not simulated.

The following GNSS constellation settings are considered:

- *Ephemeris Errors:*
  The ephemeris errors have been introduced by applying errors in downward radial direction. No along-track or across-track deviations are used. The offsets are constant over time and have zero mean and a standard deviation of 0.8 m for GPS and of 0.6 m for Galileo.
- *GPS Constellation:*
  The simulation of the GPS satellites is based on the YUMA almanac data.
- *Galileo Constellation:*
  The simulation of the Galileo satellites is based on YUMA-type almanac data.
- *RF Signal Adjustment:*
  A compensation for the higher noise temperature experienced in simulator testing compared to the usual antenna sky temperature has to be taken into account.

LION NAVIGATOR GNSS NAVIGATION PERFORMANCE IN LEO

The Low Earth Orbit allows for high performance of GNSS receivers due to the high visibility of GNSS SVs and high signal strength. It is currently the typical application for space-borne GNSS receivers. It also provides a starting point for the GTO applications both as a best possible performance reference and the comparison to the GTO perigee phase. An example of typical LEO performances of the LION Navigator is given below with < 1 m (RMS) position accuracy and < 2 mm/s (RMS) velocity accuracy in the dual frequency case.

Performance in LEO in a 600 km near circular orbit with 97° inclination was measured for three different usages of the GNSS constellations: (a) “GPS only”, (b) “Galileo only”, and (c) “GPS & Galileo”. The first three presented measurements were obtained using dual frequency, i.e. L1 C/A and L2C in case of GPS, and E1 and E5a in case of Galileo. Additional, measurements for a test mode using single frequency “GPS & Galileo” are included**.**

Table 7 provides resulting 3D RMS and standard deviation(STDV) performances, about four times better than the initial requirements. For the mostly interesting case, “GPS & Galileo” in dual frequency, further statistical evaluation is provided in Table 10 and shown in the plots for position in Figure 25 and for velocity in Figure 26.

Table 6: Performance in LEO for different test modes in 3D RMS.

Test Mode	GNSS Signal	Position [m]	Velocity [mm/s]	Pulse per Second [ns]
Dual Frequency, GPS only	L1 C/A, L2C	0.673	1.62	27
Dual Frequency, Galileo only	E1, E5a	0.870	1.19	26
Dual Frequency, GPS & Galileo	L1 C/A, L2C, E1, E5a	0.695	0.97	27
Single Frequency, GPS & Galileo	L1 C/A, E1	5.437	9.88	28

Table 7: Performance in LEO for GPS & Galileo in dual frequency (L1 C/A, L2C, E1, E5a)

	Position			Velocity		
Statistics	**Mean [m]**	**STDV [m]**	**RMS [m]**	**Mean [mm/s]**	**STDV [mm/s]**	**RMS [mm/s]**
Radial	0.046	0.460	0.462	0.00	0.84	0.84
Along-track	0.119	0.441	0.457	-0.01	0.40	0.40
Cross-track	0.005	0.246	0.246	0.03	0.27	0.27
3D	0.632	0.289	0.695	0.70	0.67	0.97

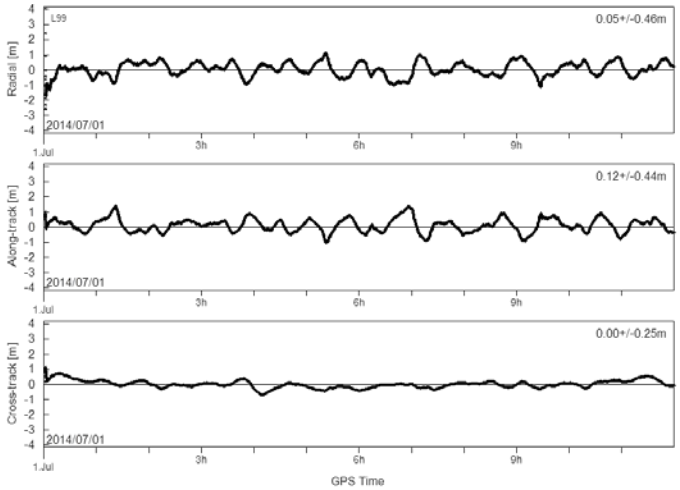

Figure 25: Position error in LEO for GPS & Galileo in dual frequency (L1 C/A, L2C, E1, E5a).

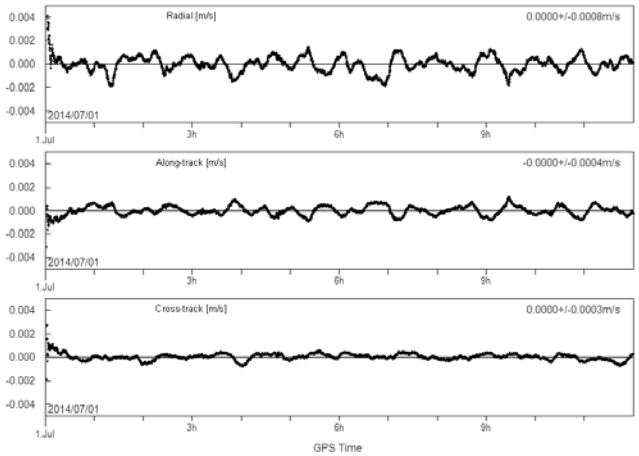

Figure 26: Velocity error in LEO for GPS & Galileo in dual frequency (L1 C/A, L2C, E1, E5a).

LION NAVIGATOR GNSS NAVIGATION PERFORMANCE IN GEO

For any satellite using a GNSS receiver for GTO the goal is to efficiently reach the designated geostationary position. Therefore – in most cases - the main mission for the GNSS receiver will be the determination of position, velocity, and time in the geostationary orbit itself. This chapter provides typical performances of the LION Navigator in GEO with < 20 m (RMS) position accuracy and <.20 mm/s (RMS) velocity accuracy.

Performance for the geostationary user was measured similar to the LEO performance tests with the difference being the user orbit and the zenith mounted receiver antenna. The same test environment was used with the same settings for signal, atmosphere, and GNSS constellations The measurements were performed for three different usages of the GNSS constellations: (a) "GPS only", (b) "Galileo only", and (c) "GPS & Galileo". The first three presented measurements were obtained using dual frequency, i.e. L1 C/A and L2C in case of GPS, and E1 and E5a in case of Galileo. Additional, measurements for single frequency GPS L1 & Galileo E1 are included demonstrating a high performance for the single frequency configuration. The achieved tracking threshold is 20 db-Hz.

Table 8 provides resulting 3D RMS performances. For the single frequency, dual constellation case, "GPS & Galileo" further statistical evaluation is provided in Table 9 and shown in the plots for position in Figure 27 and for velocity in Figure 28.

Table 8: Performance in GEO for different test modes in 3D RMS.

Test Mode	GNSS Signal	Position [m]	Velocity [mm/s]	Pulse per Second [ns]
Dual Frequency, GPS only	L1 C/A, L2C	19.42	2.76	46
Dual Frequency, Galileo only	E1, E5a	9.02	12.93	63
Dual Frequency, GPS & Galileo	L1 C/A, L2C, E1, E5a	7.58	10.03	71
Single Frequency, GPS & Galileo	L1 C/A, E1	11.58	2.17	117

Table 9: Performance in GEO for GPS & Galileo in Single Frequency (L1 C/A, E1).

	Position			Velocity		
Statistics	Mean [m]	STDV [m]	RMS [m]	Mean [mm/s]	STDV [mm/s]	RMS [mm/s]
Radial	1.17	11.39	11.44	-0.51	1.92	1.99
Along-track	1.08	0.63	1.25	0.27	0.53	0.60
Cross-track	-1.11	0.45	1.19	0.60	0.20	0.63
3D	10.32	5.24	11.58	1.77	1.24	2.17

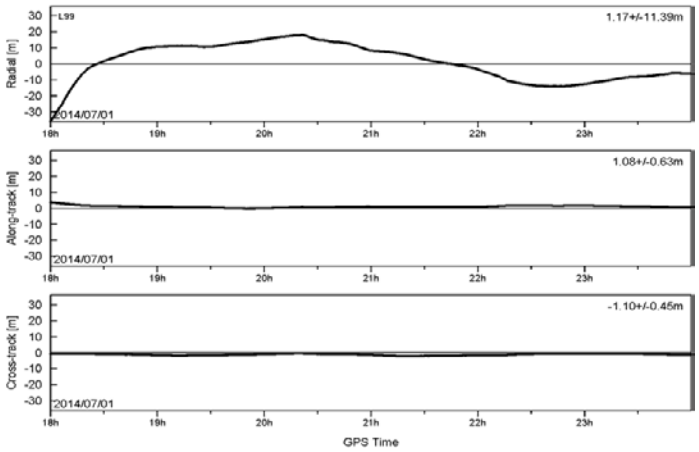

Figure 27: Position error in GEO for GPS & Galileo in single frequency (L1 C/A, E1).

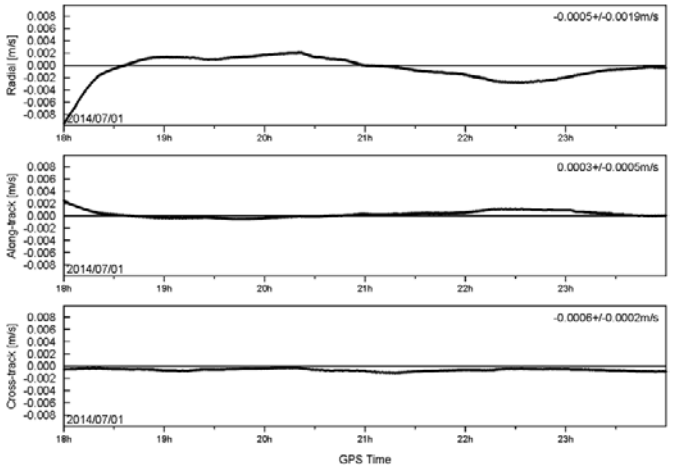

Figure 28: Velocity error in GEO for GPS & Galileo in single frequency (L1 C/A, E1).

LION NAVIGATOR IN GTO FOR ELECTRA

GTO Trajectory for Electra

Electra is an electrically powered telecommunications satellite in the sub-three-ton weight class currently being developed by OHB System AG, Germany.

The transfer to GEO with electrical propulsion is subject to ongoing investigation and optimization. Several transfer scenarios are possible, depending on the launch vehicle:

- GTO with Ariane 5 injection: The initial orbit perigee height is approx. 250 km, the apogee is approx. 35670 km (i.e. approx. GEO height).
- SSTO with Falcon 9 injection: The initial orbit perigee height is approx. 250 km, the apogee is approx. 71322 km (i.e. well above GEO height).
- Circular injection by Cyclone 4: The initial orbit perigee height is approx. 240 km, the apogee is approx. 7300 km (well below GEO height).

One likely transfer scenario for Electra is the standard GTO based on an Ariane 5 injection. This case discussed in the following. Figure 29 shows the orbit selected for GNSS navigation investigation, taken from the GTO with

Ariane 5 injection, on day one after separation from the launch vehicle. The orbit described by:

- Perigee altitude: 250 km
- Apogee altitude: 35670 km
- Inclination: 6°
- Right ascension of the ascending node: 270°
- Argument of perigee: 180°
- True anomaly: 270°

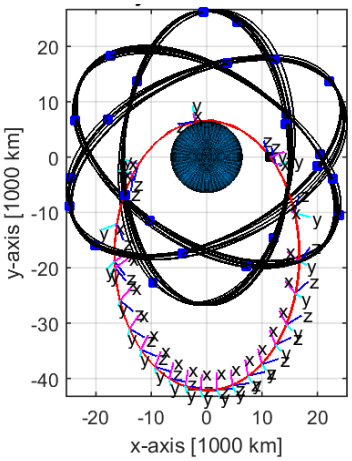

Figure 29: GTO orbit and attitude for Electra, based on Ariane 5 injection, day 1 after separation (incl. GPS orbits for comparison). Data provided by OHB Sweden.

The electrical thrusters are mounted in –z axis and provide a total, constant thrust of 540 mN in +z direction w.r.t S/C body frame.
In the following simulations and hardware-in-the-loop tests, one Rx antenna is assumed, with bore sight in +x direction w.r.t. S/C body frame. Note that this antenna placement is a trade-off made for this particular transfer scenario. As the previous visibility analyses have shown, a second Rx antenna on the +z direction provides only a very small improvement in GNSS SV visibility which does not generally justify the increase in complexity of the system.

The Electra transfer scenario data (i.e. user S/C orbit, attitude, and thrust profiles) were provided by OHB Sweden.

Simulation Results for Electra GTO
GNSS navigation simulations were performed for Electra GTO using the Airbus DS AOSE GNSS SW simulation environment and the LION Navigator [15]. The simulation uses the original LION Navigator S/W in a MATLAB/Simulink simulation environment.

The simulation was performed using the GPS and the Galileo signals L1 + E1.
The GPS constellation used for simulation has 28 SVs. This is expected to be a realistic constellation for the near future; corresponding to the current in-orbit constellation (status May 2015, with 31 active SVs), disregarding the three legacy block-IIA SVs.

The Galileo constellation used for simulation has 27 active SVs, which corresponds to the full nominal Galileo 27/9/3 Walker constellation.
Only main lobes are used for the simulations. Side lobes may improve signal availability. However, the use of side lobes needs to be further investigated before reliable statements on performance can be made, c.f. [08], [09], [10], and [11].

For the LION Navigator the following parameters were used in the simulation:

- GPS transmit power: 14.3 dBW
- Path loss (GPS Tx side): -1.5 dB
- Polarization loss: -0.5 dB
- Quantization/Sampling loss: -0.5 dB
- Additional losses (link budget contingency): -2.0 dB
- System noise temperature assumed in C/N calculation: 534 K
- Acquisition limit 27 dB-Hz
- Tracking limit 25 dB-Hz

The simulated receiver antenna pattern is derived from a space-qualified Patch-Excited Cup (PEC) antenna used on SmallGEO [22]. (Figure 30)

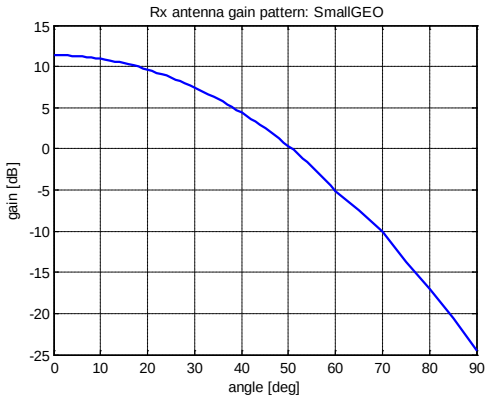

Figure 30: Rx antenna gain pattern.

Simulation results in Figure 31 show performance over two orbits for an unperturbed case, and assuming errors of 0.1% and 1 % of thrust vector command magnitude. Figure 31 shows where and how many SVs' are available and used for Kalman filter update. An update can be 13alculateed every time ≥ 2 SVs' are visible.
The Kalman filter design from LEO was used for initial tests. Even under the difficult visibility conditions of the GTO, the navigation system performed well and acted stably even under the severe perturbation of 1% thrust vector magnitude.

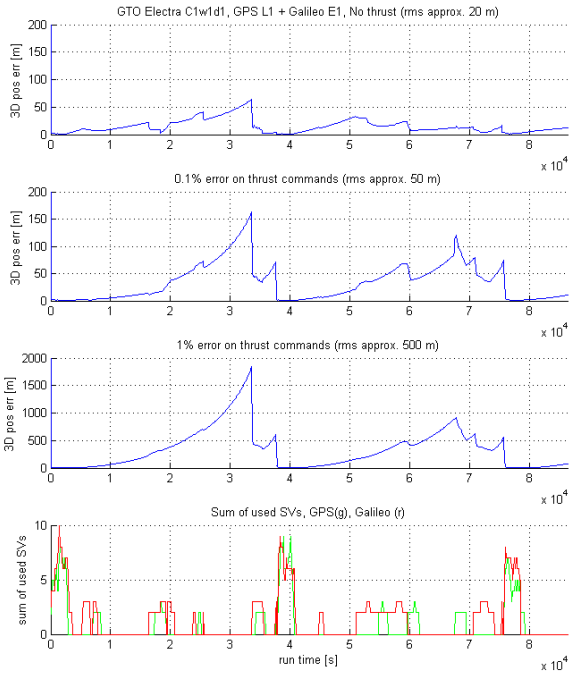

Figure 31: Simulated GNSS positioning errors for Electra GTO (Ariane 5 injection, day 1 after separation): Row 1: pos error without thrust manoeuver; Row 2: with 0.1% error on commanded thrust levels; Row 3: with 1% error on commanded thrust levels; Row 4: number of SVs used in the GNSS navigation solution (updates).

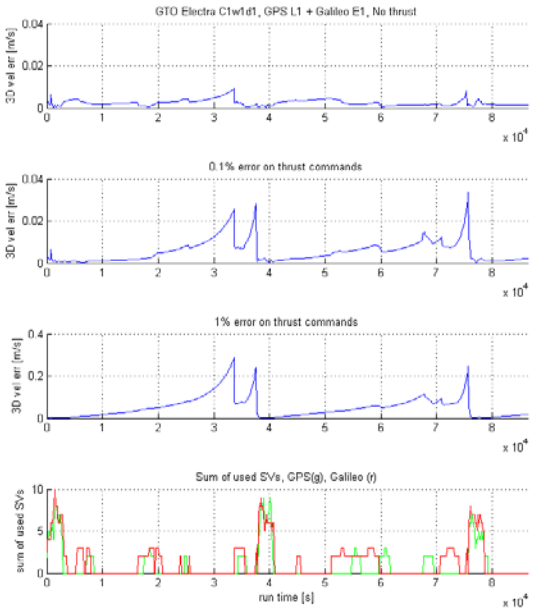

Figure 32: Simulated GNSS positioning errors for Electra GTO (Ariane 5 injection, day 1 after separation). Row 1: vel error without thrust manoeuver; Row 2: with 0.1% error on commanded thrust levels; Row 3: with 1% error on commanded thrust levels; Row 4: number of SVs used in the GNSS navigation solution (updates).

Table 10 shows the position accuracy that was achieved in simulations with and without failures in the thrust vector command.

Table 10: Simulated GNSS navigation accuracy for Electra GTO (Ariane 5 injection, day 1 after separation).

Error of thrust vector magnitude [%]	3D position error [rms]
0 (no thrust)	~20 m
0.1	~50 m
1.0	~500 m

The results show that the knowledge on the actual thrust of the electric propulsion system is the key driver of the performance here with a nearly linear relation between the accuracy of the thrust knowledge and the achievable position and velocity performance.

The Kalman filter will be further adapted to the application e.g. by extension of the state vector to include air drag, solar pressure and thrust vector misalignment and magnitude.
This will in particular make the system more tolerant against errors of the thrust vector of the electrical propulsion system. The Kalman filter is not the subject of this paper.

HW-in-the-Loop Test Results for Electra GTO

In order to demonstrate that the existing LION Navigator is able to meet the performance and be in line with the simulation results of the previous chapter, the reference orbit was formatted and transferred for the use in the Spirent simulator. The same attitude and acceleration scenario was used as in the simulation runs with an error of 1% of magnitude in the commanded thrust compared to the 'real' thrust of the reference orbit of the satellite. The test environment as described in the previous chapters was used to generate the attitude and acceleration TCs for the LION Navigator. The same parameters for the GNSS signals were used while the receiver specific losses were no longer relevant with the mathematical model of the receiver being replaced by the real hardware of the LION Navigator for this test.
The test setup is shown in Figure 24.

To further demonstrate the capabilities and possibilities for the application of the GNSS receiver for the use in electrical orbit raising to geostationary orbit a scenario with an L5-only RF front-end for the LION Navigator was selected, limiting the available GNSS signals to GPS L5 and Galileo E5 only.

Table 11: GTO Scenario Parameters.

Attitude Profile	Orbit 1 after Ariane 5 orbit injection
GPS signals	L5, 28 SVs in constellation
Galileo signals	E5a, 27 satellites in constellation
Error on thrust TCs	1% of thrust magnitude (worst case of simulations)
Rx Antenna Pattern	PEC (as simulation, c.f. Figure 30)

Table 11 shows the scenario setup for the GTO hardware-in-the-loop tests.
Figure 33 shows the achieved performance in position and velocity. The results demonstrate that the hardware tests are quite comparable with the simulations in the previous chapter with even a slightly better result in the hardware run. Figure 33 also shows the number of satellites tracked and used in the PVT calculation again showing a good correlation with the simulation.
Figure 34 and Figure 35 show the accuracy of position and velocity per axis. It can be seen that the radial axis is providing most of the error which correlates to the main direction of the electrical thrust over the orbit.

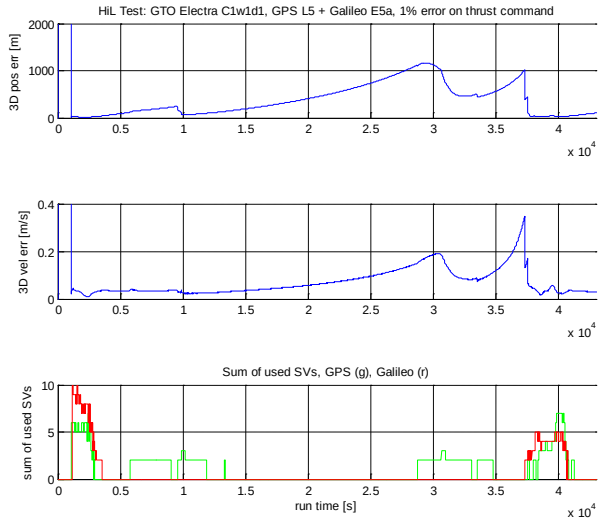

Figure 33: HiL Test Electra GTO: 3D performance in position and velocity. Number of tracked SVs (GPS: green; Galileo: red).

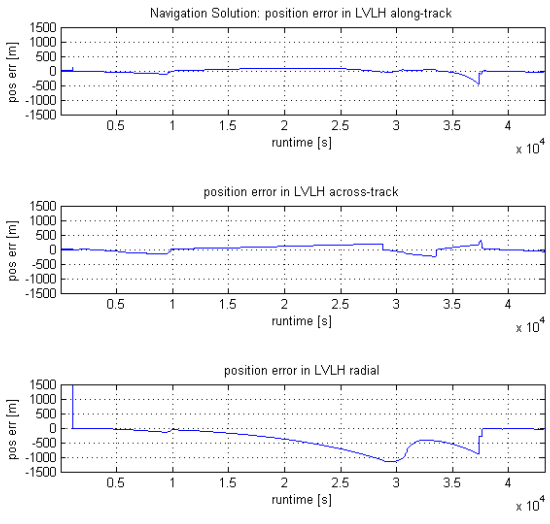

Figure 34: HiL Test Electra GTO: Position Accuracy per Axis (LVLH).

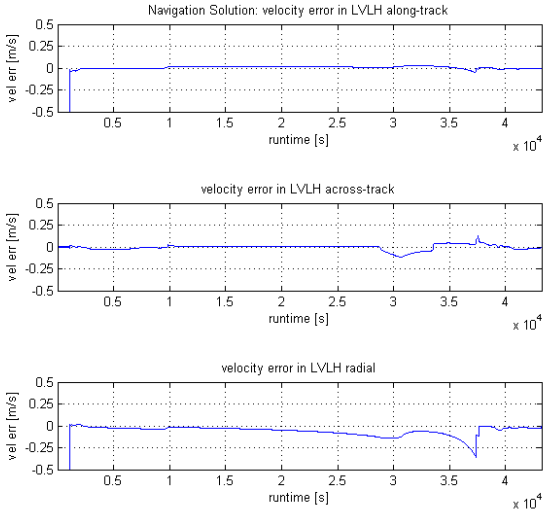

Figure 35: HiL test Electra GTO: velocity accuracy per axis (LVLH).

ALL-GNSS NAVIGATION AND ORBIT DETERMINATION

Precise orbit and position determination with centimetre accuracy is usually required for evaluation of payload data e.g. radar images. Position knowledge is also required onboard for platform operations, such as performance of station keeping manoeuvres, and determination of Earth direction from star sensor outputs for pointing of RF Payload antennas. Here an accuracy of several meters up to even hundreds of meters is mostly sufficient.

Orbit determination is conventionally done by distributed radar stations on the ground. For communication satellites, an example is two-way spread spectrum ranging (SARTRE of Timetech). For Earth observation satellites such as SPOT, the highly precise Doppler tracking system DORIS was developed.

A new approach, based solely on GPS and saving extra tracking antennas on the ground, has been successfully demonstrated for the TerraSAR-X mission [23].

TerraSAR-X is an advanced synthetic aperture radar satellite system in sun-synchronous orbit, altitude 514 km, built in public private partnership between DLR, the German Aerospace Centre, and Airbus DS GmbH.

Based on TerraSAR-X data the authors in [23] demonstrate that, using exclusively GPS data, on board autonomous navigation as well as precise post-facto orbit reconstruction is possible. To derive navigation data, TerraSAR-X is equipped with a redundant MosaicGNSS single frequency L1 receiver and the Integrated GPS Occultation Receiver (IGOR), which provides code and carrier phase measurements on L1 and L2.

The TerraSAR-X ground segment built up at the German Space Operations Centre (DLR GSOC) for precise orbit determination employs a "Reduced dynamic batch least-squares filter", designed to work with both ionosphere-free L1/L2 carrier phase data from IGOR and the ionospheric-error-free L1 code/carrier combination from MocaicGNSS receiver.

Employing the precise orbit determination system at GSOC, the authors quote a 3D RMS post-processing position accuracy of 1m for the MosaicGNSS receiver single frequency data and 5- 10cm for IGOR using L1 and L2, both from pre-mission tests.

Autonomous platform operation with the MosaicGNSS receiver is performed using an extended Kalman filter. From statistical analysis of flight results a position accuracy of 9 m 3D RMS was determined based on 200 cases of one day each.

Based on the promising results a similar approach is proposed, using onboard the LION Navigator Multi-GNSS receiver, for navigation on the transfer orbit and the final geosynchronous orbit, as backup to a fully autonomous onboard navigation solution

The two methods under discussion for orbit determination are extended Kalman filters, as in the previous sections, and weighted least squares estimation, as described for high precision orbit determination of TerraSAR-X.

Extended Kalman filters are preferred for onboard autonomous navigation since its demands on processing time and onboard memory are compatible with current onboard computer resources. In case of modelling errors, Kalman filters are vulnerable to extended data gaps (signal outages) as is shown in Figure 31 and Figure 32. The effect can be reduced by further extension and tighter tuning of the Kalman filter.

The advantage of the Least Squares approach [24] (also referred to as batch processing) is better robustness against long data gaps, which are characteristic for orbits above the constellation altitude, and smoother trajectories in general. The disadvantage is the high demand on memory and processing power, which exceeds currently available onboard resources by far.

Figure 36 shows results from an earlier study [25] based on the MosaicGNSS receiver. The figure shows a comparison between Kalman filter and batch processing performance for a geosynchronous orbit. The influence of the data gaps on the performance is clearly visible. Both methods deliver sufficiently accurate results for most platform applications. In the example, batch processing algorithms are run in a Matlab simulation environment for demonstration.

A current study aims to find the minimum number of data points required to achieve a specified accuracy to satisfy the need for most satellite platform applications, with a minimum of processing power.

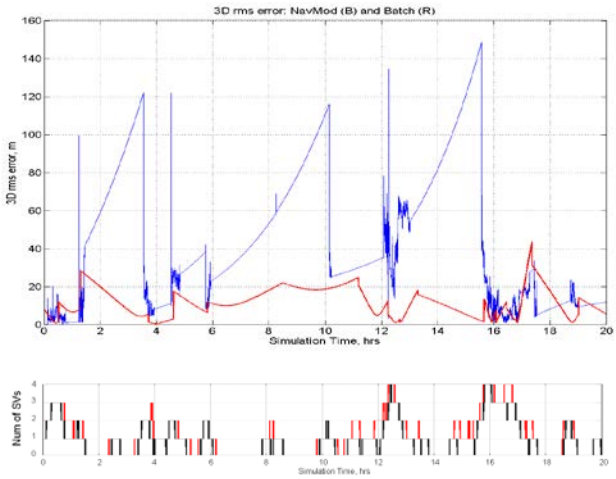

Figure 36: Batch processing performance (3D RMS error) in GEO using GPS Block IIR and 4000 measurements (red) and Kalman Filter performance (blue). Below: Number of GPS SVs that can be acquired (black) and tracked (red) [25].

CONCLUSION

All analyses and tests presented herein rely only on GNSS signals from the main lobes of the constellations as the side lobe signal quality is questionable.
The visibility analyses are based on realistic orbit and attitude profiles of electric GTO missions. They show that a second antenna will not provide significant improvements of the visibility. The link budget shows that with a typical receive antenna a tracking threshold of 22 dB-Hz provides a near complete correlation of the trackable signals to the geometrical visibility in the analyzed cases.
The Kalman filter of the LION Navigator allows for filter update with measurements from just 2 GNSS SVs providing an updated filter solution even under poor visibility conditions and propagates the solution with sophisticated orbit models during times of visibility gaps.
The simulations of the Electra case show that the main driver of the GTO performance is the knowledge about the electrical thrust. The hardware-in-the-loop tests demonstrate that the simulated performance can be achieved with the space-qualified hardware and software of the LION Navigator.

ACKNOWLEDGMENTS

The Electra GTO scenario data (i.e. user S/C orbit, attitude, and thrust profiles) were provided by OHB Sweden AB.
Additional realistic GTO scenario data were provided by Astos Solutions GmbH, Germany.
The authors thank OBH Sweden AB and Astos Solutions GmbH for their support.

GEO Performance test results were obtained within ESA contract 4000106091 “GPS/Galileo Miniaturised Space Receiver (GAMIR)” and the ESA funded study “Feasibility of GNSS Sensors for AOCS Applications in GEO and Higher Altitudes”.

REFERENCES

[01] F.H Bauer, M.C. Moreau, M.E. Dahle-Melsaether, W.P. Petrofski, B.J. Stanton, S. Thomason, A. Harris, R.P. Sena, and L. Parker Temple III., “The GPS Space Service Volume”, *Proceedings of the 19th International Technical Meeting of the Satellite Division of The Institute of Navigation. ION GNSS 2006*, September 2006, Fort Worth, Texas, USA.

[02] B. J. Stanton, L. Parker Temple III., and C. E. Edgar. “Analysis of Signal Availability in the GPS Space Service Volume. ION GNSS”, *19th International Technical Meeting of the Satellite Division of the Institute of Navigation*, Fort Worth, Texas, USA, 2006.

[03] S. Averin, V. Vinogradov, N. Ivanov, and V. Salischev. “Application of Differential Method for Relative Positioning of Geostationary Satellites with Use of GLONASS and GPS Navigation Signals.” *Proceedings of the Fifth International Conference on Differential Navigation*, 1996.

[04] O. Balbach, B. Eissfeller, G. Hein, W. Enderle, M. Schmidhuber, and N. Lemke. „Tracking GPS above GPS Satellite Altitude: Results of the GPS Experiment on the HEO Mission Equator-S.” *Position Location and Navigation Symposium*, IEEE, Palm Springs, CA, USA, 1998.

[05] J. D. Kronman, “Experience Using GPS For Orbit Determination of a Geosnychronous Satellite.” *ION GPS*, Salt Lake City, UT, USA, 2000.

[06] S. O. Erb., “High-Fidelity Optimum Electric Propulsion Transfer Design to GEO and MEO.” *64th International Astronautical Congress*, Beijing, China, 2013.

[07] S. A. Feuerborn, D. A. Neary, and J. M. Perkins. Finding a Way: Boeing's "All Electric Propulsion Satellite". *49th Joint Propulsion Conference*, San José, CA, USA, 2013.

[08] C. Frey. Evolution of GPS Capabilities, A Space Segment Perspective. *34th AAS Annual Guidance & Control Conference*, Breckenridge, CO, USA, 2011.

[09] M. Unwin, R. De Vos Van Steenwijk, P. Blunt, Y. Hashida, S. Kowaltschek, and L. Nowak. “Navigating Above the GPS Constellation - Preliminary Results from the SGR-GEO on GIOVE-A”. ION GNSS, *26th International Technical Meeting of The Satellite Division of the Institute of Navigation*, Nashville, Tennessee, USA, 2013.

[10] L. Barker, and C. Frey, “GPS at GEO: A first look at GPS from SBIRS GEO1” *35th Annual AAS Guidance and Control Conference*, Breckenridge, Colorado, USA, 2012.

[11] S. Winkler, C. Voboril, R. Hart, M. King, „GOES-R Use of GPS at GEO (Viceroy-4)“, *36th Annual AAS Guidance and Control Conference*, Breckenridge, Colorado, USA, 2013.

[12] E. Gottzein and C. Müller. ESA-Study: “Feasibility of GNSS Sensors for AOCS Applications in GEO and Higher Altitudes.” Astrium GmbH, Ottobrunn, Germany, 2011.

[13] K. Reich “GNSS Based Navigation on Transfer Orbits to Geostationary Orbit”, *Diploma Thesis, IFR University of Stuttgart*; Airbus Defence and Space, Ottobrunn, Germany; 2014.

[14] C. Kühl, H. Filippi, A. Barrios-Montalvo, P.A. Krauss, J. Heim, E. Gottzein, Astrium GmbH, Germany, “LION - A Multi Frequency, Multi Constellation Receiver for Spacecraft Navigation”, *34th AAS Guidance & Control Conference*, Breckenridge, Colorado, USA, February 2011.

[15] E. Gottzein, C. Kühl, H. Filippi, A. Barrios-Montalvo, P.A. Krauss, J. Heim, Astrium GmbH, Germany, “LION Navigator - GPS/Galileo Receiver for Spacecraft Navigation”, *24th International Technical Meeting of the Satellite Division of the Institute Of Navigation, ION GNSS 2011*, Portland, Oregon, USA,September 2011.

[16] O. Montenbruck and E. Gill, “Satellite Orbits - Models, Methods, and Applications”, Springer Verlag, 2000.

[17] GPS Interface Specification IS-GPS-200H, September 2013 (http://www.gps.gov/technical/icwg/).

[18] Galileo OS SIS ICD (Open Service Signal-In-Space Interface Control Document), Issue 1 Revision 1, September 2010 (http://ec.europa.eu/enterprise/policies/satnav/ galileo/open-service/index_en.htm).

[19] P. Misra and P. Enge. “Global Positioning System - Signals, Measurements, and Performance.” Ganga-Jamuna Press, 2011.

[20] P.A. Krauss, G. Klein, S. Sassen, Airbus Defence and Space, Germany; A. Garcia-Rodriguez, J. Roselló, European Space Agency, The Netherlands; A. Grillenberger, M. Markgraf, DLR-GSOC, Germany; A. Consoli, F. Piazza, Saphyrion, Switzerland; E. Gottzein, University Stuttgart, Germany, "GPS/Galileo Miniaturised Multi-Frequency Space Receiver (GAMIR)", *27th International Technical Meeting of the Satellite Division of the Institute Of Navigation, ION GNSS 2014*, Tampa, Florida, September 2014.

[21] P. Zentgraf et. al., "Preparing the GPS-Experiment for the Small GEO Mission", *33rd Annual AAS Guidance and Control Conference*, Breckenridge, Colorado, USA, 2010.

[22] N. Neumann, et. al., "Use of GNSS Receivers within the SmallGEO Product Line", *65th International Astronautical Congress*, Toronto, Canada, 2014.

[23] O. Montenbruck, Y. Yoon, E. Gill, M. Garcia-Fernandez: "Precise Orbit Determination for the TerraSAR-X Mission". 19th International Symposium on Space Flight Dynamics, 4-11 June 2016, Kanazawa, Japan, 2006.

[24] O. Montenbruck, T. van Helleputte, R. Kroes, E. Gill: "Reduced Dynamic Orbit Determination using GPS Code and Carrier Measurements". Aerospace Science and Technology 9, 261-371, 2005.

[25] A. Barrios-Montalvo, S. Hobbs, C.T.F. Kuehl: "In-Orbit Autonomous Position Determination of Satellites Using Sparsely Distributed GNSS Measurements: For Geostationary Transfer Orbits, Geostationary Earth Orbit and Higher Altitudes". Cranfield University, UK, 2010.

[26] AGGA-4 Datasheet AGGA4-ASTD-DS-0001.

[27] RTEMS Home Page: "www.rtems.org".